DIFFRACTION AT HERA

P. MARAGE
Université Libre de Bruxelles - CP 230, Boulevard du Triomphe
B-1050 Bruxelles, Belgium
e-mail: pmarage@ulb.ac.be

A review is presented of diffraction studies at HERA.

1 Introduction: highlights of HERA

1.1 The hard behaviour of the proton structure function F_2 at high energy

With 27.5 GeV electrons or positrons colliding with 820 or 920 GeV protons through the exchange of highly virtual photons, HERA has been since 1992 an ideal machine for studying the proton structure at very high $\gamma^* p$ centre of mass energy W (with $W^2 = y \cdot s$, $\sqrt{s}$ being the ep centre of mass energy and $0 < y < 1$) or very low x ($x \simeq Q^2/W^2$, Q^2 being the negative square of the virtual photon four-momentum).

A major discovery at HERA has been the fast rise with energy of the $\gamma^* p$ cross section or, equivalently, of the F_2 structure function, in the deep inelastic scattering (DIS) domain. This rise is larger for increasing Q^2: when the cross section at low x is parameterised as $\sigma(\gamma^* p) \propto x^{-\lambda}$, with λ depending on Q^2, $\lambda \gtrsim 0.3$ for $Q^2 \gtrsim 100$ GeV^2 [1] (*hard* behaviour), whereas $\lambda \simeq 0.08 - 0.10$ in hadron−hadron interactions [2] (*soft* behaviour).

1.2 A large diffractive component in DIS

Another major feature at HERA is the presence in the DIS domain of a large diffractive contribution, of about 8 % of the total cross section.

At high energy, diffractive and elastic scattering are governed by the exchange of the pomeron, an object carrying the vacuum quantum numbers. Pomeron exchange also governs the high energy behaviour of total hadron cross sections, which are intimately related to elastic scattering through the optical theorem. The pomeron is thus an object of fundamental importance for particle physics, and it is a major challenge for QCD to provide a detailed description of diffractive scattering in terms of quark and gluon exchange.

At HERA, by changing the intermediate photon virtuality Q^2, it is possible to vary the resolution with which the pomeron structure is probed in diffractive interactions, and to study its partonic content. HERA has thus also become a

wonderful tool for studying the QCD structure of diffraction, both providing a very rich amount of experimental results and triggering intense theoretical developments.

2 Inclusive diffraction

2.1 Kinematics

The characteristic feature of diffraction (see Fig. 1) is that the final state hadronic system is divided into two subsystems, X and Y, separated by a large gap in rapidity devoid of hadronic energy. The presence of the gap, due to the exchange of a colourless object, is attributed at high energy to pomeron exchange. In QCD, the simplest model for the pomeron is a pair of gluons.

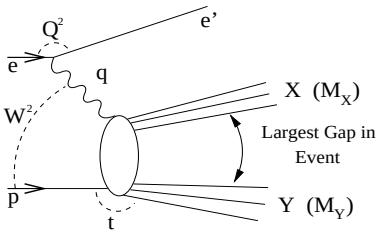

Figure 1: Deep-inelastic diffractive interaction.

When the proton remains intact ($Y = p$, "elastic" scattering), the diffractive process is defined, up to an azimuthal angle, by four kinematical variables: Q^2, $x_{I\!P}$, β and t, where t is the squared four-momentum transfer to the proton, and $x_{I\!P}$ and β are defined as

$$x_{I\!P} = 1 - x_L \simeq \frac{Q^2 + M_X^2}{Q^2 + W^2}, \quad \beta \simeq \frac{Q^2}{Q^2 + M_X^2}, \quad x = \beta \cdot x_{I\!P}, \qquad (1)$$

with x_L the fraction of the incident proton energy carried by the scattered proton; $x_{I\!P}$ is the fraction of the proton momentum carried by the exchange and β is the fraction of the exchange momentum carried by the quark struck by the photon. Kinematics imply that a gap in rapidity is created between the system X and the scattered proton when $x_{I\!P} \ll 1$, i.e. $M_X \ll W$ and $x_L \simeq 1$.

Experimentally, diffractive events are thus selected by the direct observation of a large rapidity gap in the detector [3] or, equivalently, by using the M_X distribution [4,5] and exploiting the fact that diffractive interactions are characterised by a non-exponentially suppressed rapidity gap. In both cases, a remaining background of events with proton dissociation has to be statistically subtracted, since low mass Y systems give no signal in the detectors and can not be separated from elastic proton scattering.

Diffractive events can also be selected using proton spectrometers which tag the scattered proton[6]. This provides a clean measurement of elastic diffraction without proton dissociation background, and allows a measurement of the t distribution, but the acceptance is low, especially for low $x_{I\!P}$, and the statistics accumulated so far are poor.

2.2 Diffractive structure functions

In analogy with non-diffractive DIS, the inclusive diffractive cross section is expressed in the form of a three-fold structure function (four-fold when t is measured):

$$\frac{\mathrm{d}^3\sigma\ (e+p\to e+X+p)}{\mathrm{d}Q^2\ \mathrm{d}x_{I\!P}\ \mathrm{d}\beta} = \frac{4\pi\alpha^2}{\beta Q^4}\ (1-y+\frac{y^2}{2(1+R_D)})\ F_2^{D(3)}(Q^2, x_{I\!P}, \beta), \quad (2)$$

where R_D is the ratio of the longitudinal and transverse diffractive cross sections, which has not been measured so far.

In the case of "*Regge factorisation*" [7], $F_2^{D(3)}$ can be factorised in the form

$$F_2^{D(3)}(Q^2, x_{I\!P}, \beta) = \Phi(x_{I\!P}) \cdot F_2^D(Q^2, \beta), \quad (3)$$

where $\Phi(x_{I\!P})$ can be interpreted as an effective flux. At high energy ($x_{I\!P} < 0.01$), pomeron exchange dominates, whereas for lower energy (higher $x_{I\!P}$), reggeon (ρ, ω, f mesons) exchange provides an additional significant contribution.

For fixed $x_{I\!P}$, $F_2^D(Q^2, \beta)$ describes the universal partonic structure of the exchange (*DIS factorisation*) [8], β playing the role of x for hadron structure.

Fig. 2 presents the measurement [3] of $x_{I\!P} \cdot F_2^{D(3)}$ as a function of $x_{I\!P}$ for several bins in Q^2 and β. It was fitted as the sum of a pomeron and a reggeon contribution, with possible interference [a], the fluxes being parameterised in a Regge inspired form:

$$\Phi_{I\!R,I\!P}(x_{I\!P}) \propto x_{I\!P}^{n_{I\!R,I\!P}}, \qquad n_{I\!R,I\!P} = 2 \cdot \langle \alpha_{I\!R,I\!P}(t) \rangle - 1. \quad (4)$$

An exponential t dependence, consistent with the data [9], is assumed.

In agreement with expectations, $\alpha_{I\!R}(0)$ is found to be 0.50 ± 0.18, making a significant contribution typically for $x_{I\!P} \gtrsim 0.01$. With the present statistics, the fit is not sensitive to the presence of a possible interference term.

[a] Only the f meson is expected to interfere with the pomeron.

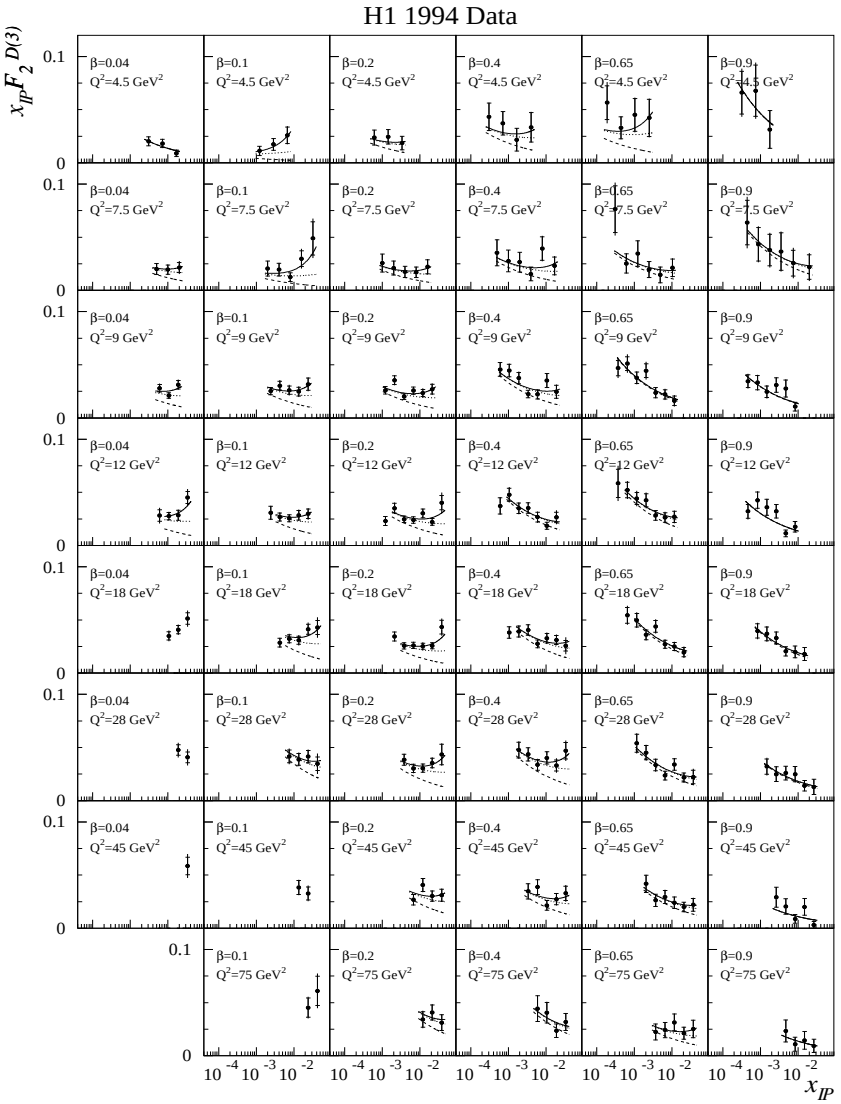

Figure 2: Measurement of $x_{I\!P} \cdot F_2^{D(3)}(Q^2, x_{I\!P}, \beta)$ ($M_Y < 1.6$ GeV, $|t| < 1$ GeV^2) as a function of $x_{I\!P}$ for various Q^2 and β values [3]. The curves show the results of the Regge fit with interference. The dashed curves show the contributions of the pomeron alone, the dotted curves, the pomeron plus interference, and the continuous curves, the total.

3 Energy dependence of diffraction; soft-hard interplay

The energy dependence of diffraction, measured by $\alpha_{I\!P}(0)$ for fixed Q^2, is shown in Fig. 3. In photoproduction [11,12], the value of $\alpha_{I\!P}(0)$ is consistent with the hadron−hadron case, as expected in view of the hadronic nature of real photons. In contrast, the measurements of $\alpha_{I\!P}(0)$ for $Q^2 \neq 0$ are significantly higher [3,4,5], indicating that naive Regge factorisation (3,4) is broken, since $\alpha_{I\!P}(0)$ depends on Q^2.

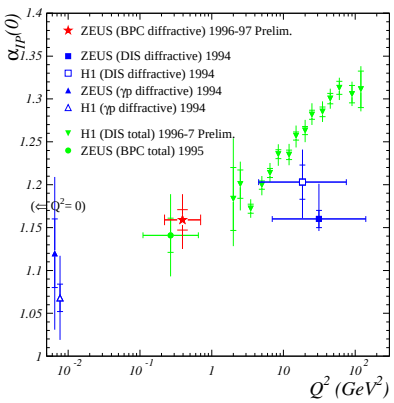

Figure 3: Measurements of $\alpha_{I\!P}(0)$ for diffractive and non-diffractive ep interactions [10].

In a QCD approach, where diffraction is attributed to parton exchange, a Q^2 dependence of $\alpha_{I\!P}(0)$ is no surprise, since parton densities at low x rise faster at higher Q^2, as measured by F_2 (see also Fig. 3). However, for a given Q^2 value, $\alpha_{I\!P}(0)$ is lower in diffraction than for inclusive DIS.

This "semi-hard" behaviour of diffraction can be most easily understood when the process is discussed in the proton rest frame [b]. In this frame, because of the large boost, the photon has time to fluctuate, far from the target, into definite hadronic states which interact diffractively with the proton: $|\gamma\rangle = |q\bar{q}\rangle + |q\bar{q}g\rangle + ...$

Two possible topologies can be contrasted:

a. The photon fluctuates into a large k_T, small transverse size dipole [c], with transverse dimension $r_\perp \propto 1/Q^2$. This large k_T topology, which implies

[b] It can be helpful when discussing diffraction to visualise the process either from the Breit frame, with emphasis on the pomeron partonic content (structure function approach), or from the proton rest frame, which insists on the hadronic fluctuations of the photon (dipole approach [13]). These complementary pictures have of course to reconcile when physical measurements are discussed.

[c] For $q\bar{q}$ fluctuations, the dipole is formed by the two quarks; in the case of $|q\bar{q}g\rangle$ fluctuations, colour factor considerations favour the topology consisting of a $(q\bar{q})$ pair opposed to the gluon.

hard scattering (as for F_2), is kinematically preferred. However, the small size of the colour dipole induces mutual screening: seen from the proton, the system appears as nearly colour neutral, and the interaction cross section is thus strongly reduced (this phenomenon is known as *colour transparency*).

b. The photon fluctuates into a longitudinally asymmetric, small k_T, large transverse size dipole ("aligned jet model"). As for hadron−hadron interactions, the cross section is large and, in the absence of a hard scale, the energy behaviour is soft, but photon fluctuations into this topology are kinematically disfavoured.

In contrast with the total cross section at high Q^2, which exhibits a purely hard behaviour, inclusive diffraction is thus a semi-hard process, which includes both a hard component (small size dipoles, kinematically preferred but damped by colour transparency) and a soft component (large size dipoles, with large cross sections but small fluctuation probabilities).

The semi-hard nature of inclusive diffraction is confirmed by the measurement of the exponentially falling t distribution: $\mathrm{d}\sigma/\mathrm{d}t \propto exp(b \cdot t)$. The ZEUS LPS measurement [9] is $b = 6.8 \pm 0.9 \pm 11$ GeV^{-2}, smaller than for soft processes ($b \simeq 10 - 12$ GeV^{-2} for ρ meson photoproduction [14,15]) but larger than for a typical hard process ($b \simeq 4 - 4.5$ GeV^{-2} for J/ψ production [16,17]).

4 Parton distributions; higher twists

In the Breit frame, the $F_2^{D(2)}$ structure function obtained from $F_2^{D(3)}$ for a fixed value of $x_{I\!P}$ describes the partonic content of the exchange. As for F_2, this structure function follows the DGLAP evolution equations, and a universal set of parton distributions can be extracted from scaling violations [d].

At a $x_{I\!P}$ value where the reggeon contribution is negligible compared to the pomeron, Fig. 4 (left) shows that scaling violations are positive even at large β, in contrast with hadron structure functions, which decrease for increasing Q^2 at large x. This suggests the presence of a large gluon component at large β in the pomeron, at variance with a very small gluon content at large x for hadrons.

Parton distributions in the pomeron, obtained from QCD fits, are shown in Fig. 4 (right). Gluons carry some 80% of the pomeron momentum, and they dominate over quarks in the full β range [e].

[d] It must be stressed that DIS factorisation applies for fixed $x_{I\!P}$ and for any mix of pomeron and reggeon in the exchange; Regge factorisation (3,4) does not have to hold.

[e] The difference between the two acceptable fits ("flat" and "peaked" gluons in Fig. 4 right) affects mostly the region with $\beta > 0.7$, which is discarded from the fit because it is affected by large higher twist effects.

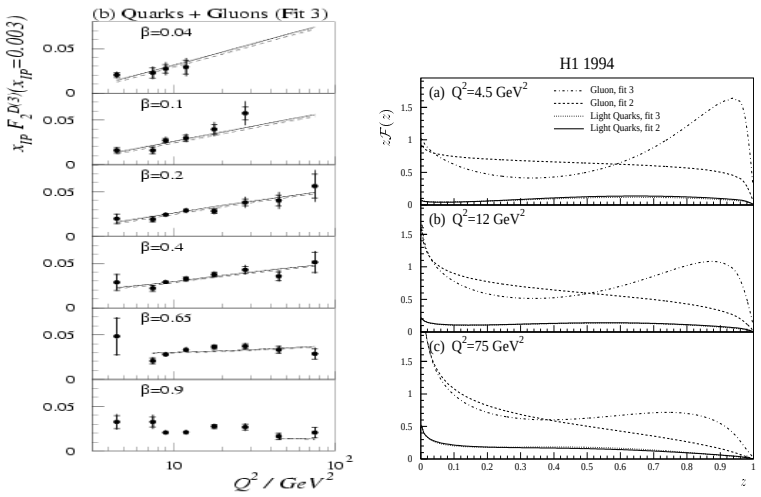

Figure 4: Left: H1 measurement of the structure function $x_{I\!P} \cdot F_2^{D(3)}$ for $x_{I\!P} = 0.003$ as a function of Q^2 in bins of β [3]; the curves are the result of a QCD fit. Right: parton distributions in the pomeron.

A specific feature of diffraction is the presence at high β of a large higher twist component, which persists for large Q^2 values. Calculations in the proton rest frame, where the pomeron is modelled as a two gluon system [18], indicate that three contributions dominate diffractive interactions: leading twist $q\bar{q}$ and $q\bar{q}g$ contributions from transverse photons, respectively in the intermediate β region and in the low β (large diffractive mass) region, and a higher twist $q\bar{q}$ contribution from longitudinal photons, dominant at large β [f]. Within measurement precision, the inclusive data agree with these predictions [4].

5 Hadronic final states

According to the DIS factorisation theorem [8], parton distributions extracted from QCD fits to inclusive diffraction can be exported to hadronic final states in DIS [g].

[f] A specific channel with a large longitudinal higher twist component is vector meson production - see section 6.

[g] It is important to note that factorisation only applies for DIS processes, and is broken for hadron−hadron interactions and for resolved photon interactions. In these cases, reinteractions between the coloured remnants during the interaction time can fill the rapidity gap, and the diffractive cross section is significantly reduced, as observed in particular at the Tevatron, when parton densities obtained at HERA are compared to diffractive dijet, W or bottom production [19].

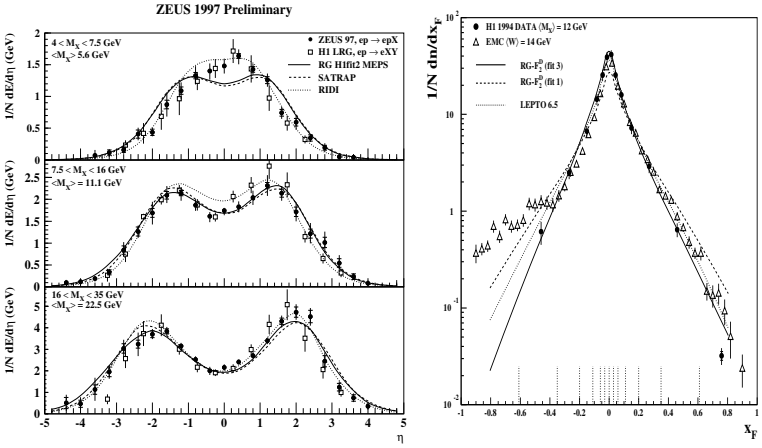

Figure 5: Left: energy flow for diffractive interactions [20]; right: x_F distribution [21]; the measurements are compared to Monte-Carlo predictions using parton distributions extracted from inclusive diffraction.

Semi-inclusive variables (energy flow, x_F, transverse momentum of tracks, multiplicity distributions) present marked differences with non-diffractive interactions, but similarities to e^+e^- annihilation. These features are reasonably well described by Monte-Carlo simulations using parton distributions otained from inclusive diffraction [20,21] – see Fig. 5.

Of particular interest is the measurement of diffractive dijet [22,23] and charm [24,25] production, since the implied boson gluon fusion process provides a direct probe of the gluon content of the pomeron.

A remarkable description of kinematical variables in diffractive dijet electroproduction [22] is achieved by a Monte-Carlo simulation which includes the H1 "flat" gluon distribution (see Fig. 6 left). An interesting feature is the broad distribution of $z_{I\!P}$, the pomeron momentum fraction carried by the two jets, and the absence of a peak for $z_{I\!P} \simeq 1$. In a Breit frame picture, this indicates the presence of pomeron remnants, as expected for a gluon dominated pomeron (see Fig. 6 d). In a proton rest frame approach, this diagram corresponds to $|q\bar{q}g\rangle$ states with a low p_T gluon (Fig. 6 c). In contrast, the contribution of large p_T, small size $|q\bar{q}\rangle$ states (Figs. 6 a) is damped by colour transparency.

For charm production, in spite of very limited statistics, similar features are observed.

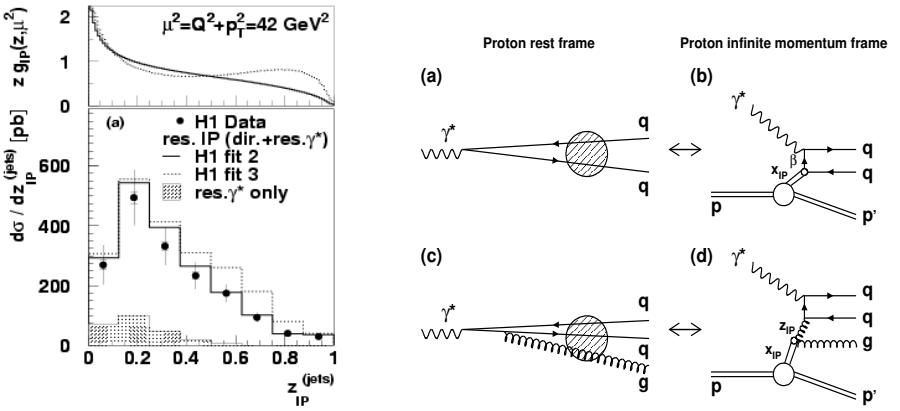

Figure 6: Left: diffractive dijet production[22] as a function of $z_{I\!P}$, compared to Monte-Carlo predictions using respectively the H1 "flat" and "peaked" gluons obtained from QCD fits to $F_2^{D(3)}$; the contribution of direct and resolved photon contributions are indicated. Right: two complementary pictures of diffractive dijet production.

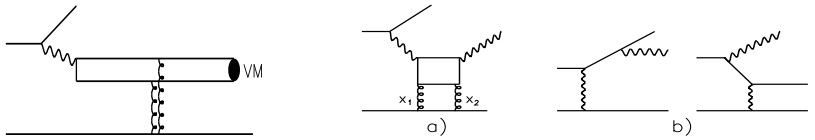

Figure 7: Left: exclusive vector meson production; right: a) deeply virtual Compton scattering; b) Bethe-Heitler (QED Compton) background to DVCS.

6 Exclusive vector particle production

The exclusive production of vector mesons and photons provides a rich diffraction laboratory: detailed studies are performed for different values of the scales provided respectively by the mass of the constituent quarks, Q^2 and t.

A striking effect is the hard energy dependence of J/ψ photoproduction [16,17] ($\alpha_{I\!P}(0) \gtrsim 0.25$), much stronger than for light vector meson photoproduction (see Fig. 8 left). This is an effect of the large charm mass, which implies that the process takes place over short distances and probes directly the hard gluon content of the proton: $\sigma(e\,p \to e\,p\,J/\psi) \propto |xG(x)|^2$. Similarly, the energy dependence of ρ and ϕ electroproduction[26,27,28] increases with Q^2.

It is remarkable that the cross sections for different vector mesons, which differ by large factors in photoproduction, are very similar, up to their quark content (SU(4) factors), once plotted as a function of $Q^2+M_V^2$ – see Fig. 8 right. This observation, in agreement with QCD expectations, confirms the role of the quark mass and of Q^2 as hard scales.

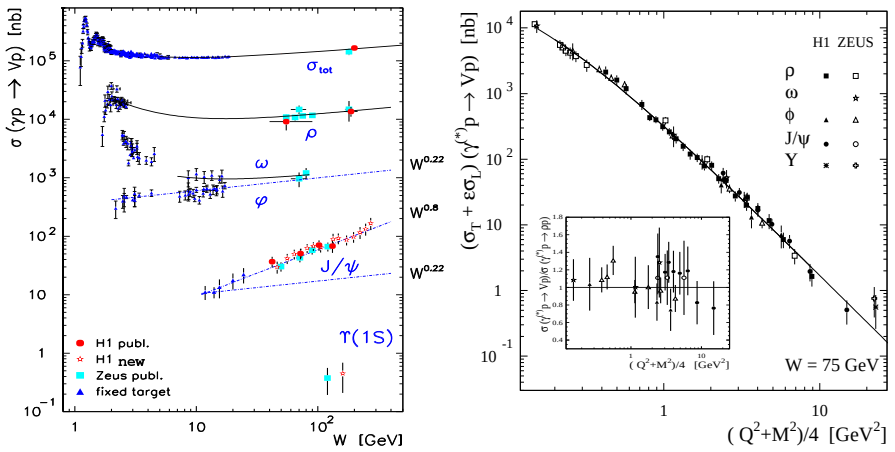

Figure 8: Left: energy dependence for $\sigma_{tot}(ep)$ and for $\rho, \omega, \phi, J/\psi$ photoproduction; right: $Q^2 + M_V^2$ dependence for photo- and electroproduction of several vector mesons, scaled by the SU(4) factors [28].

J/ψ production is also characterised [16,17] by a value of the exponential t slope $\simeq 4 - 4.5$ GeV^{-2}, much smaller than for light vector meson photoproduction. This is due to the small size of the J/ψ meson, the slope reflecting the transverse size of the interacting objects. A decrease of the slope is also observed for increasing Q^2 for ρ and ϕ mesons, with an indication of the universality of the slope as a function of $Q^2 + M_V^2$ – see Fig. 9 left.

The measurement of angular distributions for vector mesons provides information on the helicity structure of diffraction. In particular, the ratio $R = \sigma_L/\sigma_T$ of the longitudinal to transverse cross sections for ρ electroproduction increases with Q^2, as can be seen in Fig. 9 right. A small but significant violation of s-channel helicity conservation is observed [27,30], the dominant helicity flip amplitude being from a transverse photon to a longitudinal meson; this is in agreement with QCD expectations [31].

The cross section for deeply virtual Compton scattering (DVCS), where the virtual photon converts diffractively into a real photon as illustrated in Fig. 7 right a), has also been measured and found in good agreement with QCD predictions [32]. This process allows the measurement in the proton of skewed parton distributions, i.e. generalised parton distributions including correlations between partons with different longitudinal momenta. This concept [33] is introduced to describe the longitudinal momentum transfer kinematically necessary for putting on mass shell the virtual photon or the vector meson. It is also important for the photoproduction of heavy vector mesons, in particular Υ [16,34].

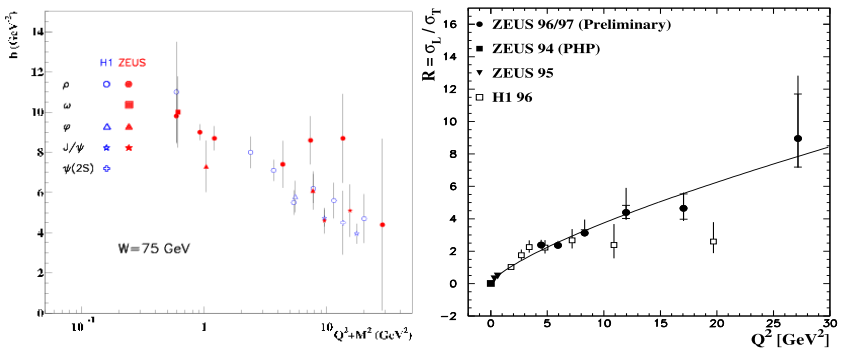

Figure 9: Left: exponential t slopes for several vector meson diffractive production, as a function of $Q^2+M_V^2$ [29]; right: $R = \sigma_L/\sigma_T$ as a function of Q^2 for ρ meson electroproduction, the curve representing an empirical fit [26].

7 Conclusions

Numerous important results on diffraction have been obtained at HERA, which triggered new theoretical developments.

However some measurements, important to test models and achieve a deeper QCD understanding of diffraction, are still missing, in particular measurements of the longitudinal cross section, of the dipole size in different processes (through measurements of the t slope) and of higher twist contributions. In addition, experimental uncertainties related to limited statistics in the presence of a hard scale (e.g. for charm production) and to the contamination of the elastic channel by proton dissociation background still affect the quality of the data.

Significant progress will be obtained from the large statistics accumulated recently and after the HERA luminosity upgrade. The installation by H1 of a very forward proton spectrometer [35] with full acceptance in t for $x_{I\!P} \simeq 0.01$ will allow clean selections of diffractive processes in the presence of a hard scale, provide measurements of the t slopes for several processes, give information on the longitudinal cross section, and open a new field of research through the comparison of elastic and proton dissociation events.

Acknowledgements

It is a pleasure to thank the organisors of the Workshop, in particular Risto Orava, for a very pleasant and fruitful meeting.

References

1. H1 Coll., S. Aid et al., *Nucl. Phys.* **B470** (1996) 3.
2. see e.g. A. Donnachie, P.V. Landshoff, *Phys. Lett.* **B296** (1992) 227.
3. H1 Coll., C. Adloff et al., *Zeit. Phys.* **C76** (1997) 613.
4. ZEUS Coll., J. Breitweg et al., *Eur. Phys. J.* **C6** (1999) 43.
5. ZEUS Coll., paper 875, ICHEP 2000, Osaka, Japan.
6. ZEUS Coll., J. Breitweg et al., *Eur. Phys. J.* **C1** (1998) 61.
7. G. Ingelman and P. Schlein, *Phys. Lett.* **B152** (1985) 256.
8. J.C. Collins, *Phys. Rev.* **D57** (1998) 3051; **D61** (2000) 019902.
9. ZEUS Coll., J. Breitweg et al., *Eur. Phys. J.* **C2** (1998) 237.
10. P. R. Newman, ICHEP 2000, Osaka, Japan.
11. H1 Coll., C. Adloff et al., *Zeit. Phys.* **C74** (1997) 221.
12. ZEUS Coll., J. Breitweg et al., *Zeit. Phys.* **C75** (1997) 421.
13. for a review, see e.g. M. F. McDermott, hep-ph/0008260 (2000).
14. H1 Coll., S. Aid et al., *Nucl. Phys.* **b463** (1996) 3.
15. ZEUS Coll., J. Breitweg et al., *Eur. Phys. J.* **C2** (1998) 247.
16. H1 Coll., C. Adloff et al., *Phys. Lett.* **B483** (2000) 23.
17. ZEUS Coll., paper 878, ICHEP 2000, Osaka, Japan.
18. J. Bartels et al., *Eur. Phys. J.* **C7** (1999) 443.
19. CDF Coll., T. Affolder et al., *Phys. Rev. Lett.* **84** (2000) 232.
20. ZEUS Coll., J. Breitweg et al., *Phys. Lett.* **B421** (1998) 368; paper 876, ICHEP 2000, Osaka, Japan.
21. H1 Coll., C. Adloff et al., *Eur. Phys. J.* **C1** (1998) 495; *Phys. Lett.* **B428** (1998) 206; *Eur. Phys. J.* **C5** (1998) 439.
22. H1 Coll., C. Adloff et al., hep-ex/0012051.
23. ZEUS Coll., J. Breitweg et al., *Eur. Phys. J.* **C5** (1998) 41.
24. ZEUS Coll., paper 874, ICHEP 2000, Osaka, Japan.
25. H1 Coll., paper 157ag, HEP99, Tampere, Finland.
26. ZEUS Coll., paper 880, ICHEP 2000, Osaka, Japan.
27. H1 Coll., C. Adloff et al., *Eur. Phys. J.* **C13** (2000) 371.
28. H1 Coll., C. Adloff et al., *Phys. Lett.* **B483** (2000) 360.
29. R. Yoshida, RADCOR 2000, Carmel, USA.
30. ZEUS Coll., J. Breitweg et al., *Eur. Phys. J.* **C12** (2000) 393.
31. D. Yu. Ivanov and R. Kirschner, *Phys. Rev.* **D58** (1998) 114026.
32. H1 Coll., paper 966, ICHEP 2000, Osaka, Japan.
33. see e.g. A. V. Radyushkin, *Phys. Rev.* **D56** (1997) 5524.
34. ZEUS Coll., J. Breitweg et al., *Phys. Lett.* **B487** (1998) 432.
35. http://web.iihe.ac.be/h1pot/